

# Estimation of switching characteristics in quantum-dot cellular automata using probability model

Chen Xiangye<sup>1</sup>, Cai Li<sup>1</sup>, Jia Kaixiang<sup>2</sup>, Yao Xiaokuo<sup>1</sup>, Zhang Mingliang<sup>1</sup>

<sup>1</sup>College of Science, Air Force Engineering University, Xi'an 710051, People's Republic of China

<sup>2</sup>Polytechnic College, Xi'an University of Science and Technology, Xi'an 710054, People's Republic of China  
E-mail: 852340691@qq.com

Published in Micro & Nano Letters; Received on 25th September 2013; Accepted on 10th December 2013

Quantum-dot cellular automata (QCA) is a novel computational paradigm which utilises the quantum mechanism to encode and process bit information. The switching characteristics of the QCA majority gate are evaluated by using the proposed probability model. All kinds of probabilities are achieved by solving the time-independent Schrodinger equation. The simulation results reveal that the majority gate switches at a higher correct probability when the cell distance and the size decrease. Cell miniaturisation would raise a significant implication in how to realise reliable QCA fabrication. In addition, the results also illuminate that majority output has different probabilities when the inputs change. Therefore, to analyse the QCA circuit reliability by using the probability model, all the input combinations must be considered.

**1. Introduction:** The conventional transistor based on CMOS technology faces great challenges as it was predicted as Moor's Law [1, 2]. Bottlenecks, such as quantum effects, short channel effects, integration and power dissipation, may hinder further progress in scaling microelectronics [1, 2]. Quantum-dot cellular automata (QCA) is a new paradigm, which encodes the binary information with Coloumbic interaction instead of current switching [3, 4]. Such characteristics make it possible to achieve circuit densities and clock frequencies beyond the limits of the existing CMOS technology [5–7]. QCA is regarded as one of the candidates to replace modern silicon circuitry [5–7]. In the QCA cells, Coloumbic interaction between cells is sufficient to accomplish the computation, and there are no current flows among the cells [3, 8, 9]. Features such as low power dissipation, high device density and high switching speed, were presented by the QCA, and attracted much attention.

Nanoelectronic systems are extremely likely to demonstrate high defects and fault rates [10–12]. As a nanoelectronic system, the QCA are also faced with the challenge of providing reliable computation. A high percentage of probabilistic errors have been shown because of factors like engineering techniques and signal noise [13–16]. As a quantum device, to characterise the reliability of the QCA circuits, it is not sufficient only to specify just the binary states (0 or 1) of the individual cells, but also the probabilities of being in these states. Largely, for this reason, the probability models have been studied by a number of research groups with different methods. Patel presented probabilistic transfer matrix (PTM) for tolerance analysis at the circuit level [17]. Krishnaswamy *et al.* [18] employed algebraic decision diagrams to improve the efficiency of the PTM operations. Ganesh showed interest in the Bayesian networks (BNs) for obtaining the probability of correct output at the logic level [19]. Thara and Sanjukta [20] formed a complete joint probability model for probabilistic computing. However, to our knowledge, how the cell size and the cell–cell distance affect the switching characteristics has not received much attention.

As demonstrated in this Letter, a vast amount of work has been conducted in order to study the relationship between the QCA switching characteristics and the cell size. We founded the Bayesian model of the majority with the Bayesian radius  $r = 2$ . To study the relation between the inputs and the switching probabilities clearly, simulations with different inputs are performed by utilising the probability model. The probabilistic model has demonstrated its validity by its nonlinear response and rapid

saturation, which are consistent with the cell–cell response function presented in previous works. The simulations also reveal that the majority gate will switch more reliably when the cell size and the distance become smaller. The results would raise a significant implication in how to realise reliable QCA fabrication.

The rest of the Letter is organised as follows. Section 2 provides the application of the BNs theory to the QCA devices. The model of the majority gate Bayesian is shown in Section 3. Section 4 presents the computation of the condition probability. In Section 5, the simulation results are shown and analysed. Section 6 concludes this Letter.

**2. Bayesian model for computation:** Fig. 1a shows a QCA wire with five cells shown in,  $\{x_1, x_2, x_3, \dots, x_5\}$ .  $r$  denotes the Bayesian radius. The foregoing cells marked as  $x_i, x_{i+1}, x_{i+2}, \dots, x_{i+r-1}$  are the inputs, and  $x_{i+r}$  is the output. Each cell can be observed to be in two possible states: 0, or 1 [3]. The probability of state 0 is donated by  $P\{x_i = 0\}$ , and for 1, by  $P\{x_i = 1\}$ .

BNs are graphical probabilistic models representing the joint probability function over a set of random variables by using a directed acyclic graphical (DAG) structure [20]. The nodes describe the random variables, and the node to node arrowheads denote the direct causal dependencies. For a linear arrangement of the five QCA cells shown in Fig. 1b, keeping the Bayesian radius as  $r = 1$ , the exact joint probability distribution can be given by the following equation

$$\begin{aligned}
 &P\{x_5 = 1, x_4 = 1, \dots, x_1 = 1\} \\
 &= P\{x_5 = 1|x_4 = 1\} \cdot P\{x_4 = 1|x_3 = 1\} \\
 &\cdot P\{x_3 = 1|x_2 = 1\} \cdot P\{x_2 = 1|x_1 = 1\} \cdot P\{x_1 = 1\} \quad (1)
 \end{aligned}$$

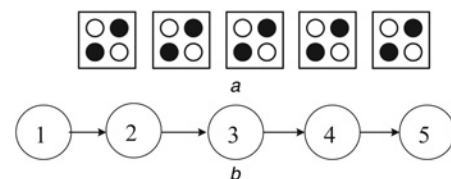


**Figure 1** QCA wire  
a QCA layout  
b Bayesian model

**3. Majority model:** It is a notable characteristic that the quantum devices work based on quantum effects instead of statistical theories. As for the majority, the quantum effects are shown by a phenomenon where the correct probability of the output varies when the inputs do not remain the same. By taking the majority, for example, when the inputs change from '000' to '001', the correct probability of the output does change at some degree though the output remains at state '0'. There are eight kinds of inputs for the majority, hence eight kinds of correct probabilities of output exist. However, in fact we only need one correct probability. The simplest way to obtain the probability is to compute the mean of the eight probabilities.

$P\{X_7=1\}$ ,  $P\{X_8=1\}$  and  $P\{X_9=1\}$  are the probabilities where  $x_7$ ,  $x_8$  and  $x_9$  stay at the correct state. These probabilities will become more accurate if the Bayesian radius increases. However, most of the previous reports utilised BNs with radius  $r=1$ . In this Letter, to balance the operational complexity and the precision, the Bayesian radius is taken as  $r=2$ . Fig. 2 shows the Bayesian model for the BN analysing to calculate the proper probability.  $P\{X_7=1\}$ ,  $P\{X_8=1\}$  and  $P\{X_9=1\}$  can be achieved

$$P\{X_7=1\} = \sum_{i=1}^{64} P\{x_7=A|\text{eve}7_i\} \cdot P\{\text{eve}7_i\} \quad (2)$$

$$P\{X_8=1\} = \sum_{i=1}^{16} P\{x_7=A|\text{eve}8_i\} \cdot P\{\text{eve}8_i\} \quad (3)$$

$$P\{X_9=1\} = \sum_{i=1}^4 P\{x_7=A|\text{eve}9_i\} \cdot P\{\text{eve}9_i\} \quad (4)$$

There are six cells that can perturb  $x_7$ , marked as  $\{x_1, x_2, x_3, x_4, x_5, x_6\}$ .  $\{x_1, x_3, x_5\}$  act as fixed cells. Hence, the amount of the events is  $2^3=8$ .  $\text{eve}7_i$  is one of the events. To simplify the computation, only eight events were taken into consideration:  $\{0, 0, 0, 0, 0, 0\}$ ,  $\{0, 0, 0, 1, 0, 0\}$ ,  $\{0, 1, 0, 0, 0, 0\}$ ,  $\{0, 1, 0, 1, 0, 0\}$ ,  $\{0, 0, 0, 0, 0, 1\}$ ,  $\{0, 0, 0, 1, 0, 1\}$ ,  $\{0, 1, 0, 0, 0, 1\}$  and  $\{0, 1, 0, 1, 0, 1\}$  (here,  $\{0, 0, 0, 0, 0, 0\}$  is corresponding to  $\{x_1=0, x_2=0, x_3=0, x_4=0, x_5=0, x_6=0\}$ ).

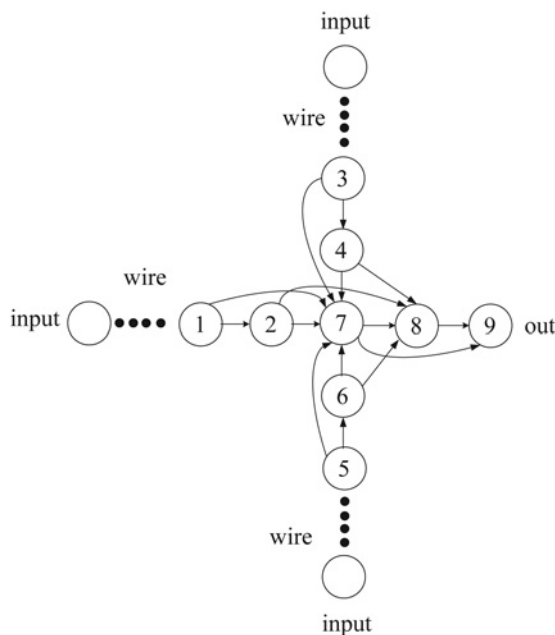


Figure 2 Bayesian model of the majority

Hence, (2) can be modified as

$$\begin{aligned} P\{X_7=1\} = & P\{x_7=1|111100\} \cdot P\{111100\} \\ & + P\{x_7=1|111111\} \cdot P\{111111\} \\ & + P\{x_7=0|001100\} \cdot P\{001100\} \\ & + P\{x_7=1|001111\} \cdot P\{001111\} \\ & + P\{x_7=0|110000\} \cdot P\{110000\} \\ & + P\{x_7=1|110011\} \cdot P\{110011\} \\ & + P\{x_7=0|000000\} \cdot P\{000000\} \\ & + P\{x_7=0|000011\} \cdot P\{000011\} \end{aligned} \quad (5)$$

Here,  $P\{x_7=0|000000\}$  corresponds to  $P\{x_7=0|x_1=0, x_2=0, x_3=0, x_4=0, x_5=0, x_6=0\}$ . Obviously,  $\{x_1=0, x_2=0\}$ ,  $\{x_3=0, x_4=0\}$  and  $\{x_5=0, x_6=0\}$  are independent of each other, and exploit an approximate arithmetic,  $P\{x_1=0, x_2=0\}$ ,  $P\{x_3=0, x_4=0\}$  and  $P\{x_5=0, x_6=0\}$  are close to  $P\{x_1=0\}$ ,  $P\{x_3=0\}$  and  $P\{x_5=0\}$ . Hence, (5) is equal to

$$\begin{aligned} P\{X_7=1\} = & P\{x_7=0|000000\} \cdot P\{x_2=0\} \\ & \cdot P\{x_4=0\} \cdot P\{x_6=0\} \\ & + P\{x_7=0|000011\} \cdot P\{x_2=0\} \\ & \cdot P\{x_4=0\} \cdot P\{x_6=1\} \\ & + P\{x_7=0|001100\} \cdot P\{x_2=0\} \\ & \cdot P\{x_4=1\} \cdot P\{x_6=0\} \\ & + P\{x_7=1|001111\} \cdot P\{x_2=0\} \\ & \cdot P\{x_4=1\} \cdot P\{x_6=1\} \\ & + P\{x_7=0|110000\} \cdot P\{x_2=1\} \\ & \cdot P\{x_4=0\} \cdot P\{x_6=0\} \\ & + P\{x_7=1|110011\} \cdot P\{x_2=1\} \\ & \cdot P\{x_4=0\} \cdot P\{x_6=1\} \\ & + P\{x_7=1|111100\} \cdot P\{x_2=1\} \\ & \cdot P\{x_4=1\} \cdot P\{x_6=0\} \\ & + P\{x_7=1|111111\} \cdot P\{x_2=1\} \\ & \cdot P\{x_4=1\} \cdot P\{x_6=1\} \end{aligned} \quad (6)$$

$P\{x_1=0\}$ ,  $P\{x_3=0\}$  and  $P\{x_5=0\}$  are the correct probabilities of the three inputs. As for  $x_8$ , by adopting the conclusion to deal with (2), we have

$$\begin{aligned} P\{X_8=1\} = & P\{x_8=0|0000\} \cdot P\{x_7=0|000\} \\ & \cdot P\{x_2=0\} \cdot P\{x_4=0\} \cdot P\{x_6=0\} \\ & + P\{x_8=0|0010\} \cdot P\{x_7=1|001\} \\ & \cdot P\{x_2=0\} \cdot P\{x_4=0\} \cdot P\{x_6=1\} \\ & + P\{x_8=0|0100\} \cdot P\{x_7=1|010\} \\ & \cdot P\{x_2=0\} \cdot P\{x_4=1\} \cdot P\{x_6=0\} \\ & + P\{x_8=1|0111\} \cdot P\{x_7=1|011\} \\ & \cdot P\{x_2=1\} \cdot P\{x_4=1\} \cdot P\{x_6=0\} \\ & + P\{x_8=0|1000\} \cdot P\{x_7=1|100\} \\ & \cdot P\{x_2=1\} \cdot P\{x_4=0\} \cdot P\{x_6=0\} \\ & + P\{x_8=1|1011\} \cdot P\{x_7=1|101\} \\ & \cdot P\{x_2=1\} \cdot P\{x_4=0\} \cdot P\{x_6=1\} \\ & + P\{x_8=1|1101\} \cdot P\{x_7=1|110\} \\ & \cdot P\{x_2=1\} \cdot P\{x_4=1\} \cdot P\{x_6=0\} \\ & + P\{x_8=1|1111\} \cdot P\{x_7=1|111\} \\ & \cdot P\{x_2=1\} \cdot P\{x_4=1\} \cdot P\{x_6=1\} \end{aligned} \quad (7)$$

where  $P\{x_8 = 0|0000\}$  is corresponding to  $P\{x_8 = 0|x_2 = 0, x_4 = 0, x_6 = 0, x_7 = 0\}$ , and  $P\{x_7 = 0|000\}$  is corresponding to  $P\{x_7 = 0|x_2 = 0, x_4 = 0, x_6 = 0\}$ , and as for  $x_9$ , there is

$$P\{X_9 = 1\} = P\{x_9 = 0|00\} \cdot P\{00\} + P\{x_9 = 0|11\} \cdot P\{11\} \quad (8)$$

$P\{x_9 = 0|00\}$  is the same as  $P\{x_9 = 0|x_7 = 0, x_8 = 0\}$ .  $P\{X_9 = 1\}$  is the probability needed radically.

**4. Condition probabilities computing:** In the preceding Section, condition probabilities are needed to compute  $P\{X_7 = 1\}$ ,  $P\{X_8 = 1\}$  and  $P\{X_9 = 1\}$ .  $P\{x_7 = 0|000\}$  is calculated as an example in this Section. The Hamiltonian of  $x_7$  is

$$H_7^{\text{cell}} = H_0^{\text{cell}} + H^{\text{kink}} \quad (9)$$

$H_0^{\text{cell}}$  is the Hamiltonian of an isolated cell [21].  $H^{\text{kink}}$  is the Hamiltonian donated by  $x_2, x_4$  and  $x_6$

$$H^{\text{kink}} = \begin{bmatrix} -E_{\text{kink}}^{2,7} & -E_{\text{kink}}^{4,7} & -E_{\text{kink}}^{6,7} & 0 \\ 0 & E_{\text{kink}}^{2,7} + E_{\text{kink}}^{4,7} + E_{\text{kink}}^{6,7} & & \end{bmatrix} \quad (10)$$

$E_{\text{kink}}^{2,7}$ ,  $E_{\text{kink}}^{4,7}$  and  $E_{\text{kink}}^{6,7}$  are the kink energies and  $E_{\text{kink}}^{2,7}$  can be gained as follows

$$E_{\text{kink}}^{2,7} = E_{\text{opposite polarisation}}^{2,7} - E_{\text{same polarisation}}^{2,7} \quad (11)$$

$E_{\text{opposite polarisation}}^{2,7}$  stands for the Coulombic potential energy because of the electrons of  $x_2$  and  $x_7$  when they have the same polarisation, and the  $E_{\text{same polarisation}}^{2,7}$  represents the Coulombic potential energy caused by the electrons of  $x_2$  and  $x_7$  when they have the opposite polarisation. A time-independent Schrodinger equation is used to achieve the states of  $x_7$ . The ground state is corresponding to the lower energy.  $|\mathfrak{S}_0\rangle$  is represented in this basis as

$$|\mathfrak{S}_0\rangle = \alpha \cdot |\phi_1\rangle + \beta \cdot |\phi_2\rangle \quad (12)$$

$|\phi_1\rangle$  and  $|\phi_2\rangle$  are the basis vectors of the QCA [7]. In the QCA structures, since the information is stored in the physical systems close to their ground states, the coefficients are valuable for the

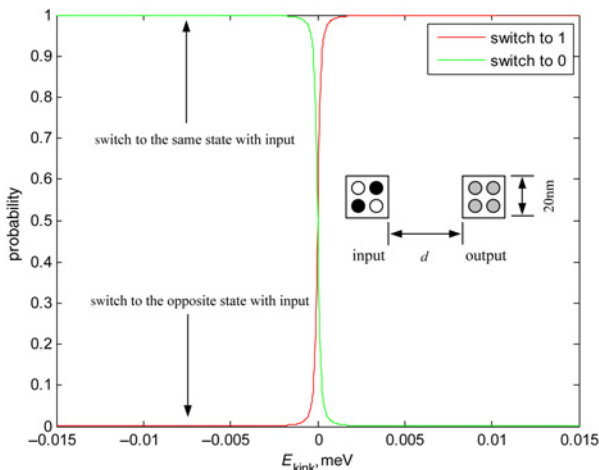


**Figure 3** Cell switching probabilities response to the kink energy nonlinearly

condition probabilities computation

$$\alpha^2 = P\{x_7 = 0|x_2x_4x_6\} \quad (13)$$

$$\beta^2 = P\{x_7 = 1|x_2x_4x_6\} \quad (14)$$

## 5. Simulation and analysis

**5.1. Switching probabilities dependence on the kink energy:** It has been proved that the polarisation of one cell is strongly coupled to the polarisation of the neighbouring cell [3]. The probability model must demonstrate its validity by computing consistent simulation results with the previous research. We show in the inset of Fig. 3 that two nearby cells are taken into consideration. The cell size is 20 nm. Assume that the input polarisation is fixed at 1 or 0. The probabilities of the output cell being at 1 or 0 are computed as the distance ( $d$ ) between the input and the output ranges. Fig. 3 reveals that very tiny kink energies can cause the output cell to switch to the same state as the input cell at probabilities of about 100%. As the Figure shows, the probabilities saturate very quickly. This nonlinear response and the rapid saturation are consistent with the cell–cell response function presented by Lent, which proves the validity of the probability model proposed.

**5.2. Switching probabilities of the majority:** The probability model is performed to gain the probabilities of  $x_7, x_8$  and  $x_9$  being at each

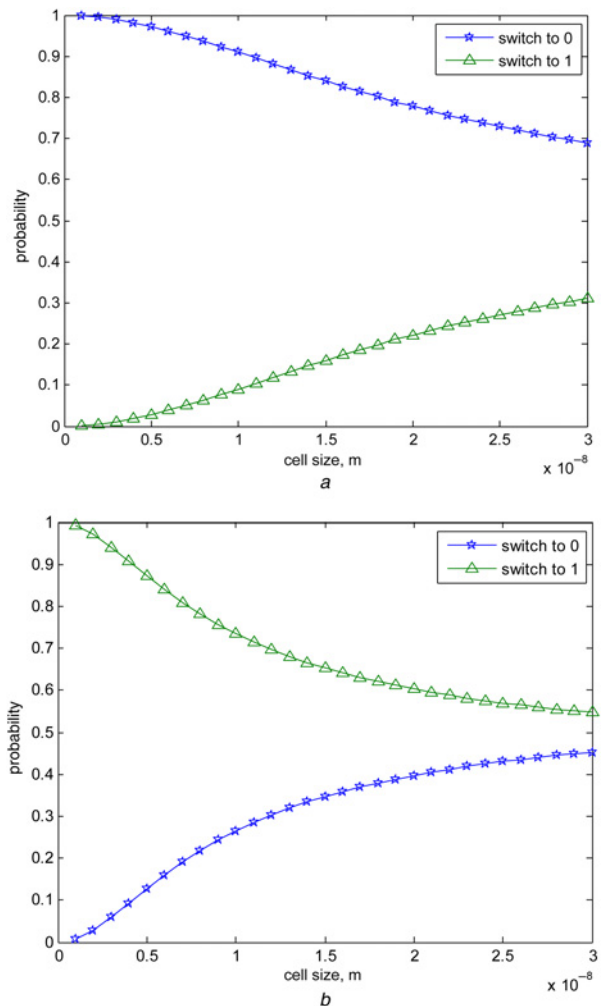


**Figure 4** Switching probabilities of  $x_9$   
a Inputs 000  
b Inputs 111

state as discussed in Section 3. Here, our main concern is the probabilities of  $x_9$  and the relationship between the output probability and the cell size. Some universal parameters are taken as follows:  $E_0 = -4$  meV,  $\gamma = 0.3$  meV, the distance between the two cells is two times the cell size,  $\epsilon_r = 10$ .

Fig. 4a shows that  $x_9$  has a higher probability to stay at state 0 when the majority has an input 000. However, this probability decreases as the cell size increases. This is quite acceptable; the cell–cell Coulomb coupling becomes stronger when the cell size and the distance become smaller. According to the nonlinear function presented in Fig. 3, the condition probabilities will go higher along with the cell size and the decreasing distance, which results in  $x_9$  having a higher probability to stay at state 0.

To study the relation between the inputs and the switching probabilities clearly, another simulation was performed by utilising the probability model. Fig. 4b shows that  $x_9$  has different probabilities to stay at state 1 when the majority inputs change to 111. In Fig. 4a, the cell size is 20 nm, and  $x_9$  will be 0 with the probability at 80%. Although the inputs change to 111,  $x_9$  will be 1 with the probability at 62%. This is because different inputs donate different kink energies to  $x_8$  and  $x_9$ . Hence, the Hamiltonian of the output cell does not remain invariable. According to the results in Section 4, the output cell gains different probabilities when the Hamiltonian changes. Thus, to analyse the QCA circuit reliability by using the probability model, all the input combinations must be considered.

**6. Conclusions:** In this Letter, the method for the QCA switching characteristics probabilistic model, has been developed. In addition, the characteristics of the majority gate with different inputs are studied. A few observations and conclusions based on the experimental simulations are as follows:

1. The probabilistic model has been proposed as a method to analyse the QCA cell's switching. The probabilistic model has demonstrated its validity by its nonlinear response and rapid saturation, which are consistent with the cell–cell response function presented in previous works.

2. The probabilities of the majority output being at 0 or 1 have been computed by using the probability model. The simulations reveal that the majority gate will switch more reliably when the cell size and the distance become smaller. Cell miniaturisation would raise a significant implication in how to realise reliable QCA fabrication.

3. The probability model also illuminates that the majority output has different probabilities when the inputs change. Thus, to analyse the QCA circuit reliability by using the probability model, all the input combinations must be considered.

**7. Acknowledgments:** This work was supported in part by the National Natural Science Foundation of China under grant no. 61172043 and in part by the Key Program of Shanxi Provincial

Natural Science Foundation for Basic Research under grant no. 2011JJZ015.

## 8 References

- [1] Peercy P.S.: 'The drive to miniaturization', *Nature*, 2000, **406**, pp. 1023–1026
- [2] Meindl J.D.: 'Beyond Moore's Law: the interconnect era'. *Comp. Sci. Eng.*, 2003, January/February, **5**, pp. 20–24
- [3] Lent C.S., Tougaw P.D., Porod W., *ET AL.*: 'Quantum cellular automata', *Nanotechnology*, 1993, **4**, (1), pp. 49–57
- [4] Tougaw P.D., Lent C.S.: 'Logical devices implemented using quantum cellular automata'. *Appl. Phys.*, 1994, **75**, pp. 1818–1825
- [5] Thapliyal H., Ranganathan N., Kotiyal S.: 'Design of testable reversible sequential circuits'. *IEEE Trans. Very Large Scale Integr. (VLSI) Syst.*, 2012, **21**, pp. 1201–1209 doi:10.1109/TVLSI.2012.2209688
- [6] ITRS: 'International technology roadmap for semiconductors 2006 update edition'. Technical report, ITRS, 2011
- [7] Tougaw P., Lent C.: 'Dynamic behavior of quantum cellular automata', *J. Appl. Phys.*, 1996, **80**, (8), pp. 4722–4736
- [8] Lent C.S., Tougaw P.D.: 'A device architecture for computing with quantum dots', *Proc. IEEE*, 1997, **85**, (4), pp. 541–557
- [9] Pudi V., Sridharan K.: 'Low complexity design of ripple carry and Brent-Kung adders in QCA', *IEEE Trans. Nanotechnol.*, 2012, **11**, (1), pp. 105–119
- [10] Jie H., Taylor E., Gao J., Fortes J.: 'Faults, error bounds and reliability of nanoelectronic circuits'. *Proc. 16th Int. Conf. on Application-Specific Systems, Architecture and Processors*, Samos, Greece, 2005, pp. 247–253
- [11] Timothy J., Dysart P.M., *ET AL.*: 'Reliability impact of n-modular redundancy in QCA', *IEEE Trans. Nanotechnol.*, 2011, **10**, (5), pp. 1105–1122
- [12] Bhaduri D., Shukla S., Graham P., *ET AL.*: 'Comparing reliability-redundancy tradeoffs for two Von Neumann multiplexing architectures', *IEEE Trans. Nanotechnol.*, 2007, **6**, (3), pp. 265–279
- [13] Beckett P., Jennings A.: 'Towards nanocomputer architecture'. *Proc. 7th Asia-Pacific Conf. Computer Systems Architecture*, Melbourne, Australia, 2002, pp. 141–150
- [14] Nikolic K., Sadek A., Forshaw M.: 'Architectures for reliable computing with unreliable nanodevices'. *Proc. IEEE Nano'01*, Maui, HI, USA, 2001, pp. 254–259
- [15] Heath J., Kuekes P., Snider G., Williams R.: 'A defect tolerant computer architecture: opportunities for nanotechnology', *Science*, 1998, **80**, pp. 1716–1721
- [16] Goldstein S.C., Budiu M.: 'Nanofabrics: spatial computing using molecular electronics'. *Proc. Annual Int. Symp. Computer Architecture (ISCA)*, Goteborg, Sweden, 2001, pp. 178–189
- [17] Patel K.N., Markov I.L., Hayes J.P.: 'Evaluating circuit reliability under probabilistic gate-level fault models'. *Proc. Int. Workshop Logic Synthesis (IWLS'30)*, Laguna Beach, CA, USA, 2003, pp. 59–65
- [18] Krishnaswamy S., Markov I.L., Hayes J.P.: 'Accurate reliability evaluation and enhancement via probabilistic transfer matrices'. *Proc. of Conf. on Design Automation and Test in Europe*, Munich, Germany, 2005, pp. 282–287
- [19] Sanjukta B., Sudeep S.: 'Probabilistic modeling of QCA circuits using Bayesian networks', *IEEE Trans. Nanotechnol.*, 2006, **5**, (6), pp. 657–670
- [20] Thara R., Sanjukta B.: 'Scalable probabilistic computing models using Bayesian networks'. *Circuits and Systems*, 48th Midwest Symp., Covington, England, 2005, pp. 712–715
- [21] Timler J., Lent C.S.: 'Power gain and dissipation in quantum-dot cellular automata', *J. Appl. Phys.*, 2002, **91**, (2), pp. 823–831